Electronic Supplementary Material (ESI) for Physical Chemistry Chemical Physics.

Supporting Information

Dysprosium-doped iron oxide nanoparticles boosting spin-spin relaxation: computational and experimental study

Jinchang Yin,‡[a] Feihong Xu,‡[a] Hongbin Qu,[a] Chaorui Li,[a] Shiyi Liu,[a] Lizhi Liu[b] and Yuanzhi Shao*[,a]

[a.] School of Physics, State Key Laboratory of Optoelectronic Materials and Technologies, Sun Yat-sen University, Guangzhou, 510275, P. R. China.

*E-mail: stssyz@mail.sysu.edu.cn

[b.] Center of Medical Imaging and Image-guided Therapy, Sun Yat-sen University Cancer Center, State Key Laboratory of Oncology in South China, Collaborative Innovation Center for Cancer Medicine, Guangzhou 510060, P. R. China.

‡ Jinchang Yin and Feihong Xu contributed equally to this work.

The explicit formula of the T_2 relaxation rate r_2 depending upon the saturation magnetization M_s

The explicit formula was provided by Bao[S1,S2]:

$$r_2 = \left(\frac{256\pi^2\gamma^2}{405}\right)\kappa M_s^2 R^2/[D\left(1+\frac{L}{R}\right)], \qquad \text{(S1)}$$

where γ is the proton gyromagnetic ratio, M_s is saturation magnetization and R is effective radius of magnetic nanostructure. L is the thickness of an impermeable surface coating. D is the diffusivity of water, and κ is the conversion factor. In Gillis's model, all electronic spins are aligned and therefore crystal magnetic moment is N times of the individual electronic magnetic moment. N is the number of electrons in the crystal.

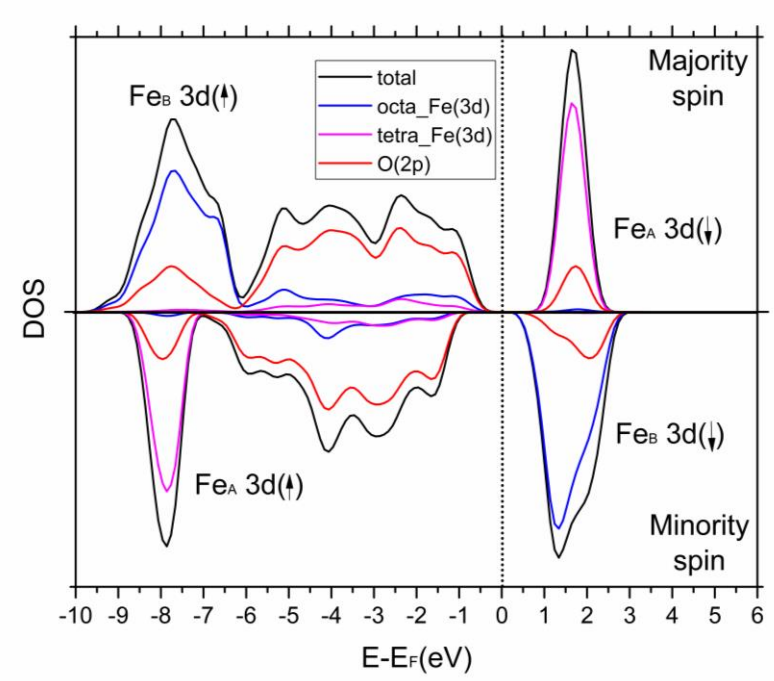

Figure S1. Electronic density of states of γ-Fe_2O_3 with inverse spinel structure. Its projection over Fe 3d and O 2p orbitals is drawn. The magnetic moments on octahedral sites (in blue) and tetrahedral sites (in pink) are oriented in opposite directions. The majority part is set to positive, while the minority DOS is set to negative. The vertical short dashed line shows the Fermi energy of the system.

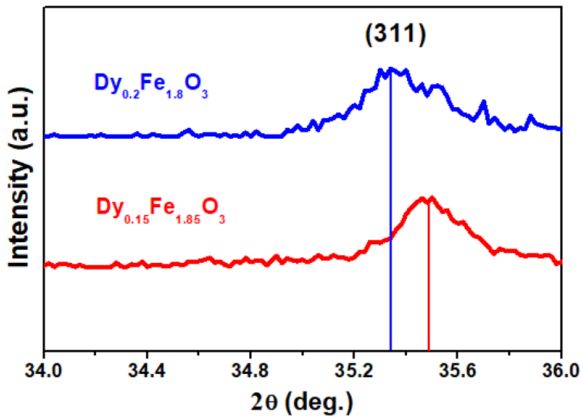

Figure S2. X-ray diffraction patterns of the Dy-doped γ-Fe_2O_3 nanoparticles at 7.5% (optimal doping) and 10%, respectively.

Figure S2 shows that the diffraction angle decreases slightly with increasing dysprosium content over the optimal doping. Based on the Bragg equation: $2dsin\theta = n\lambda$, it is able to figure out that the interplanar spacing increases with doping dysprosium accordingly. Dysprosium ion has a much larger radius than iron does; therefore replacement of iron with dysprosium over the optimal doping amount brings about lattice expansion and distortion of γ-Fe_2O_3.

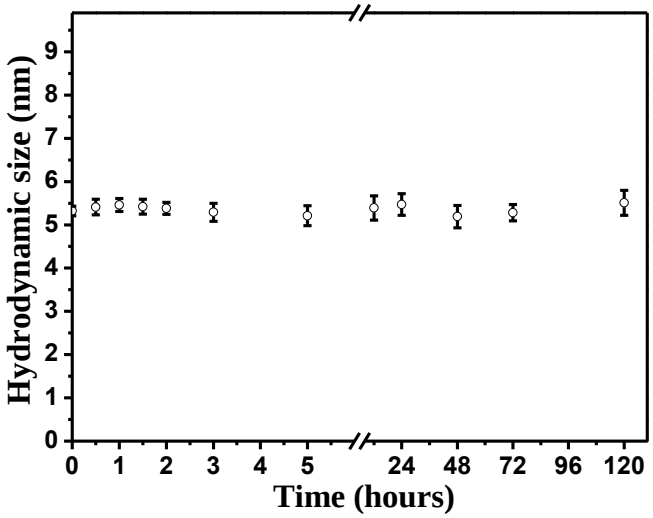

Figure S3. Size variation curve of PEG-coated Dy-doped γ-IOSNPs dispersed in aqueous solution at different temporal points, suggesting a good colloidal stability.

Table S1. Comparison of the conventional T_2 contrast agents and the designed iron oxide nanoprobes for MRI

Contrast agents	Particle size (nm) [a]	Surface coating	r_2 [b] (mM^{-1} s^{-1})	B_0 [c] (T)	Ref.
Feridex (Fe_3O_4; γ-Fe_2O_3)[d]	4.96	dextran	41	1.5	S3
Resovist (Fe_3O_4)	4	carboxydextran	61	1.5	S3
Ferumoxtran (Fe_3O_4; γ-Fe_2O_3)[d]	4.5	dextran + citrate	66	1.4	S4
VSOP (Fe_3O_4; γ-Fe_2O_3)[d]	4	citrate	32	1.5	S5
Supravist (Fe_3O_4; γ-Fe_2O_3)[d]	3-5	carbodextran	57	1.5	S6
MION (Fe_3O_4)	4.6	dextran	34.8	0.47	S7
ESION (γ-Fe_2O_3)	3	PEG[e]	29.2	3	S8
GdIO (Fe_3O_4 + Gd_2O_3)[f]	3.5	dopamine sulfonate	34.38	0.5	S9
GdIO (Fe_3O_4 + Gd_2O_3)[f]	4.8	dopamine sulfonate	41.14	0.5	S9
Fe_3O_4-PEG350	4	PEG350	39	1.4	S10
Fe_3O_4-PEG1100	4	PEG1100	17.5	1.4	S10
γ-IOSNPs (γ-Fe_2O_3)	4.15	short chain HOOC-PEG-COOH	67.8	1.5	this work
Dy-doped γ-IOSNPs ($Dy_{0.15}Fe_{1.85}O_3$)	4.15	short chain HOOC-PEG-COOH	123.2	1.5	this work

[a] The particle size is the size of magnetic particle under TEM observations without surface coating. [b] r_2: spin-spin relaxivity or transerse relaxivity. [c] B_0: magnetic field strength. [d] Crystal structure of magnetic particle is not demonstrated clearly. [e] PEG: polyethylene glycol. [f] Gd_2O_3 is embedded in Fe_3O_4 particles.

References

S1 Z. Zhou; R. Tian; Z. Wang; Z. Yang; Y. Liu; G. Liu; R. Wang; J. Gao; J. Song; L. Nie; X. Chen, *Nat. Commun.*, 2017, **8**, 15468.

S2 S. Tong, S. Hou, Z. Zheng, J. Zhou and G. Bao, *Nano Lett.*, 2010, **10**, 4607-4613.

S3 M. Rohrer, H. Bauer, J. Mintorovitch, M. Requardt, and H. Weinmann, *Invest. Radiol.*, 2005, **40**, 11.

S4 Z. Zhao, Z. Zhou, J. Bao, Z. Wang, J. Hu, X. Chi, K. Ni, R. Wang, X. Chen, Z. Chen and J. Gao, *Nat. Commun.*, 2013, **4**, 2266.

S5 M. F. Casula, P. Floris, C. Innocenti, A. Lascialfari, M. Marinone, M. Corti, R. A. Sperling, W. J. Parak and C. Sangregorio, *Chem. Mater.*, 2017, **22**, 1739-1748.

S6 H. Wei, O. T. Bruns, M. G. Kaul, E. C. Hansen, M. Barch, A. Wisniowska, O. Chen, Y. Chen, N. Li, S. Okada, J. M. Cordero, M. Heine, C. T. Farrar, D. M. Montana, G. Adam, H. Ittrich, A. Jasanoff, P. Nielsen and M. G. Bawendi, *Proc. Natl. Acad. Sci. U. S. A.*, 2017, **114**, 2325-2330.

S7 N. Chan, M. Laprise-Pelletier, P. Chevallier, A. Bianchi, M. A. Fortin and J. K. Oh, *Biomacromolecules*, 2014, **15**, 2146-2156.
S8 W. Lee., S. H. Son, B. Jin, J. Na, S. Kim, K. Kim, E. E. Kim, Y. G. Yu, and H. H. Lee. *Proc. Natl. Acad. Sci. U. S. A.,*2013, **110**, 48.
S9 Z. Zhou,. L. Wang, X. Chi, J. Bao, L. Yang, W. Zhao, Z. Chen, X. Wang, X. Chen,and J. Gao, *ACS Nano*, 2013, **7**, 32887-3296.
S10 U. I. Tromsdorf, O. T. Bruns, S. C. Salmen, U. Beisiegel, and H. Weller, *Nano Lett.*,2009, **9**, 4434-4440.